

Quantifying the Generalization Gap: A New Benchmark for Out-of-Distribution Graph-Based Android Malware Classification

Ngoc N. Tran
Vanderbilt University
Nashville, TN, USA

Anwar Said
Vanderbilt University
Nashville, TN, USA

Waseem Abbas
The University of Texas at Dallas
Richardson, TX, USA

Tyler Derr
Vanderbilt University
Nashville, TN, USA

Xenofon D. Koutsoukos
Vanderbilt University
Nashville, TN, USA

Abstract

While graph-based Android malware classifiers achieve over 94% accuracy on standard benchmarks, they exhibit a significant generalization gap under distribution shift, suffering up to 45% performance degradation when encountering unseen malware variants from known families. This work systematically investigates this critical yet overlooked challenge for real-world deployment by introducing a benchmarking suite designed to simulate two prevalent scenarios: MalNet-Tiny-Common for covariate shift, and MalNet-Tiny-Distinct for domain shift. Furthermore, we identify an inherent limitation in existing benchmarks where the inputs are structure-only function call graphs, which fails to capture the latent semantic patterns necessary for robust generalization. To verify this, we construct a semantic enrichment framework that augments the original topology with function-level attributes, including lightweight metadata and LLM-based code embeddings. By providing this expanded feature set, we aim to equip future research with richer behavioral information to facilitate the development of more sophisticated detection techniques. Empirical evaluations confirm the effectiveness of our data-centric methodology, with which classification performs better under distribution shift compared to model-based approaches, and consistently further enhances robustness when used in conjunction. We release our precomputed datasets, along with an extensible implementation of our comprehensive pipeline, to lay the groundwork for building resilient malware detection systems for evolving threat environments.

CCS Concepts

• Security and privacy → Malware and its mitigation; • Computing methodologies → Machine learning; Natural language processing.

Keywords

malware classification, distribution shift, graph neural networks

1 Introduction

Android malware continues to evolve rapidly, posing persistent challenges to the reliability and robustness of automated detection systems. Recent advances in graph-based learning have led to promising approaches for malware classification by representing applications as *function call graphs* (FCGs), where nodes correspond to individual functions and directed edges represent invocation relationships [26, 33, 58]. Graph Neural Networks (GNNs) [23, 35]

applied to these graphs enable the modeling of structural and behavioral patterns that are indicative of malicious behavior [36]. Compared to image-based approaches like byteplot representations [17], graph-based methods provide a more interpretable, semantically structured, and functionally meaningful abstraction.

Graph-based malware classification gained momentum with the release of MalNet [16], a large-scale dataset of over 1.5 million Android malware samples represented as FCGs. A smaller, balanced subset named MalNet-Tiny was released to support benchmarking. Since then, MalNet-Tiny has become a standard for evaluating GNN architectures, with state-of-the-art models achieving over 94% accuracy [46, 47]. However, these results often assume standard data splits. Recent work [55] shows that performance drops significantly when evaluating models on samples from malware families not seen during training, highlighting a critical weakness under distribution shift. As prior research mostly focuses on achieving the highest accuracy on a well-conditioned dataset, this gap in robustness has been largely overlooked in the literature, severely limiting the practical deployment of graph-based classifiers in real-world scenarios where new unseen malware variants frequently emerge.

To investigate this issue, we construct and release two new benchmark variants of MalNet-Tiny for evaluating robustness under distribution shifts. In *MalNet-Tiny-Common*, training and test samples are drawn from overlapping malware families but different subtypes, simulating the *covariance shift* scenario where novel approaches to an existing attack paradigm are encountered. For *MalNet-Tiny-Distinct*, test samples originate from families unseen during training [55], replicating the *domain shift* problem when completely unknown malware families often come up in practice. We thoroughly benchmark several state-of-the-art GNN architectures on these datasets, and evaluate the performance under distribution shift of existing solutions to domain generalization, to present the current development landscape.

Another key limitation underlying this sensitivity to distribution shifts is the lack of semantic information in MalNet-Tiny. During graph construction, all function-level data (e.g., names, types, code) was removed to avoid exposing potentially sensitive artifacts [16]. While this decision aimed to reduce reverse-engineering risks, we argue it unnecessarily restricts the model’s ability to reason about functional behavior. First, the full malware binaries used to generate these graphs are publicly available [2, 17]. Second, prior work has shown that semantic features can be integrated without compromising security [3, 58]. Moreover, we hypothesize that this omission impairs generalization for FCGs, whose edges denote information

flow rather than structural similarity. In such graphs, node semantics are essential for effective message passing and representation learning [23, 29]. Without them, models tend to memorize local structures that do not transfer well across malware families.

Motivated by this insight, our second contribution proposes an enhanced attributed graph construction framework tailored for Android malware classification under distribution shift. Our method enriches each FCG with semantic node features extracted directly from the malware’s code. Specifically, we extract a set of lightweight, widely available metadata features—including function names, signatures, access flags, instruction statistics, and Android-specific behaviors commonly used in malware analysis [3, 58]. When decompiled source code is available, we embed function bodies using a large language model (LLM), providing dense representations of behavioral semantics. These semantic vectors are combined with standard structural features and injected as node attributes for downstream GNNs. Importantly, our framework is designed for real-world deployment scenarios, where semantic features may be partially missing. To address this, we introduce three collation strategies—*Trim*, *Zero*, and *Prune*—that transform partially defined graphs into a consistent format suitable for learning. We find that our proposed semantic graph construction significantly improves classification accuracy under both settings. These results highlight the critical role of semantic information in improving the generalization of graph-based malware classifiers under novel threats.

In summary, our key contributions are as follows:

- We identify and demonstrate the brittleness of state-of-the-art graph-based Android malware classifiers under distribution shift, where detection accuracy drops sharply on test samples drawn from previously unseen malware families.
- We construct and release two new benchmark datasets, *MalNet-Tiny-Common* and *MalNet-Tiny-Distinct*, designed to evaluate classifier robustness under different types of distribution shifts.
- We propose a semantic feature enrichment framework for Android FCGs that augments structural graphs with function metadata and LLM-derived embeddings. To address real-world data quality challenges where semantic features may be inconsistently available, we introduce three collation strategies that robustly transform incomplete graphs into usable inputs for GNNs.
- We evaluate the performance of different GNN architectures and training strategies on the new datasets with/without our proposed semantic graph representations, empirically demonstrating the effectiveness of semantic features against distribution shift when combined with adaptation-based training.

The code and datasets are available at <https://ngoc.io/malnet-features>.

Differences from existing datasets. There are very limited number of datasets for Android malwares available on the internet, especially when some cannot be found [1] or explicitly taken down [60]. Most existing datasets extract features on a sample level [4, 6, 7, 40], and/or lacked reproducible process for future feature engineering. Others [17, 41] represent malwares as byteplots, effectively posing malware classification as an image classification task, and thus do not leverage the inherent structure of the input. Closest to our work, [20, 25] have contributed datasets on *concept drift*, where the definition of malwares changes over time; however, this direction is orthogonal to our versions of distribution shift. Moreover,

these datasets also only extracted features on the sample level; and with unevenly distributed classes, they create additional challenges for continuing experimentation. To the best of our knowledge, our work is the first to contribute distribution-shifted datasets for graph-based Android malware classification. We present additional related works in Section D of the Appendix.

2 Preliminaries

2.1 MalNet and Graph-Based Malware Data

MalNet [16] is a large-scale dataset of Android malware samples, where each sample is represented as a FCG extracted using AndroGuard [12]. Each node in the FCG corresponds to a function, and edges indicate function calls. Labels are derived from VirusTotal reports and unified into a hierarchy of malware *families* and *types* using Euphony [30]. A cleaned and balanced subset, MalNet-Tiny, was introduced to support manageable training and evaluation, with each class defined by a unique (family, type) pair. A more detailed discussion on MalNet is shown in Appendix A.1.

2.2 Distribution Shift in Malware Classification

We consider a standard supervised classification setting, where each malware sample is denoted by X , and its associated label by Y . The training data is drawn from a source distribution \mathcal{D} , while test-time samples may be drawn from a different target distribution \mathcal{D}' . *Distribution shift* then refers to the condition where the distributions of training and testing data differ, leading to a performance drop during model evaluation. While there are many types of distribution shifts [45], we focus only on settings where labels for malwares do not change, i.e. $\mathbb{P}_{(X,Y)\sim\mathcal{D}}(Y|X) = \mathbb{P}_{(X,Y)\sim\mathcal{D}'}(Y|X)$. Among them, *covariate shift* happens when malwares of the same labels are collected from different sources, meaning $\mathbb{P}_{\mathcal{D}}(Y) = \mathbb{P}_{\mathcal{D}'}(Y)$ but $\mathbb{P}_{\mathcal{D}}(X) \neq \mathbb{P}_{\mathcal{D}'}(X)$. *Domain shift* is a more general form of distribution shift where the training and test data come from completely different distributions, i.e. $\mathbb{P}_{\mathcal{D}}(Y) \neq \mathbb{P}_{\mathcal{D}'}(Y)$ and $\mathbb{P}_{\mathcal{D}}(X) \neq \mathbb{P}_{\mathcal{D}'}(X)$. *Temporal shift* is similar to covariate shift, but differs in that the distribution mismatch is caused by malwares changing over time.

2.3 Research Objectives

Malware classifiers must remain effective under distribution shift, as new variants often differ from prior data. Our goal is to provide a qualitative benchmark to examine this problem, and identify potential factors that contribute to it. To support this, we introduce two MalNet-Tiny-style datasets simulating covariate and domain shifts for robust evaluation, and propose a framework that enhances attributed graph construction, mitigates data-quality issues, and incorporates distribution-aware graph learning.

3 Constructing Distribution-Shifted Datasets

In this section, we describe the construction of our new benchmark datasets. Recall that each malware label in MalNet-Tiny is a malware *family/type* pair, where *family* is a broader category of malwares with similar characteristics, and *type* is a subcategory within a family. Leveraging this hierarchical labeling, we construct new datasets from the original MalNet to realistically simulate different distribution shifts from MalNet-Tiny: MalNet-Tiny-Common for covariate shift, and MalNet-Tiny-Distinct for domain shift. These datasets are curated to have these same properties for both compatibility

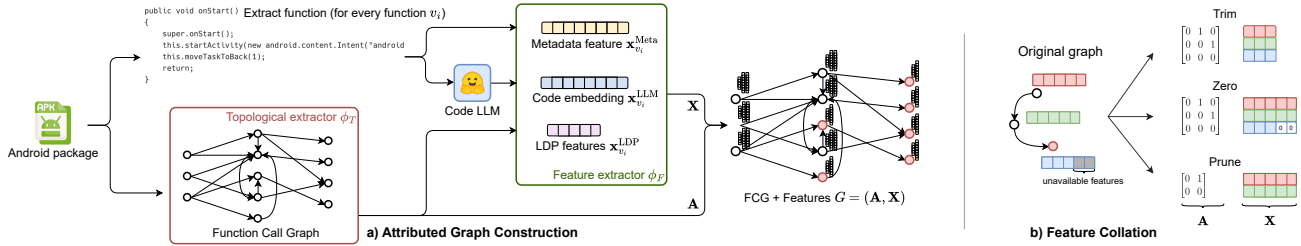


Fig. 1: Overview of the robust graph learning pipeline. For each Android package, we (a) extract and merge the FCG structure and semantic function features into a complete attributed graph, where red nodes indicate unavailable features (Sec. 4.2); then (b) make sure all input graphs with missing features are model-ready (Sec. 4.3).

Tab. 1: Malware labels of MalNet-Tiny variants (family/type).

MalNet-Tiny	MNT-Common	MNT-Distinct
addisplay / kuguo	addisplay / dowgin	spr / lootor
adware / airpush	adware / startapp	clicker+trj / dowgin
benign / benign	benign / benign	riskware / nandrobox
downloader / jiagu	downloader / mixed	malware / mixed
trojan / artemis	trojan / deng	spyware / mixed

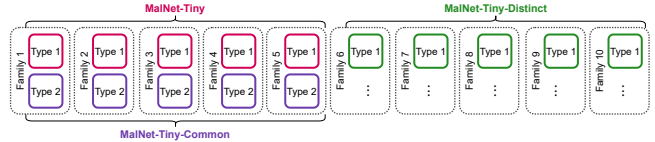


Fig. 2: Diagram of the dataset labels. Dashed boxes (columns) denote malware families, solid box denotes types/classes.

and a fair comparison with the baselines. Malware families/types and their corresponding samples are selected to be as disjoint as possible, with the chosen labels listed in Tab. 1. Fig. 2 visualizes the relationships between the labels across datasets. We also intended to create a dataset for temporal shift, but were unable to do so due to MalNet having too few malwares belonging to MalNet-Tiny classes despite its large size. While we believe our proposed method is also robust to temporal shift, we leave this as a future work.

3.1 Covariate Shift: MalNet-Tiny-Common

We construct MalNet-Tiny-Common to have the same malware families but different malware types to MalNet-Tiny to simulate a covariate shift scenario. The label correlation between the two datasets let us alternatively interpret the training process as fitting malwares to their corresponding family labels instead of types, implying that a model trained on MalNet-Tiny can be used as-is to classify MalNet-Tiny-Common, but performance will drop due to the distribution shift. For the sampling process, we seed all random sampling with 0. We start by sampling types from the same families as MalNet-Tiny, and then sample 1,000 samples from each type. The two exceptions to the label selection are: (i) the unchanged benign class is sampled from a disjoint set of malware samples, and (ii) the *downloader* family included multiple malware types, as it does not have any other one type with 1,000 qualifying samples.

3.2 Domain Shift: MalNet-Tiny-Distinct

The construction process for MalNet-Tiny-Distinct is similar to MalNet-Tiny-Common, but with different malware families/types to simulate domain shift. This dataset is designed to test the ability of adaptation schemes to generalize to completely new malwares, and is expected to be more challenging than MalNet-Tiny-Common. However, even with the large size of the original MalNet, and to

the best of our effort sampling data from as disjoint malware families/types as possible, the labels for MalNet-Tiny-Distinct are noisier than which of other variants, with more generic families and more mixed labels. The full list of malware families/types for all datasets is listed in Tab. 7 in the Appendix.

4 Feature Construction and Data Processing

As hypothesized in Sec. 1, we believe that the lack of semantic information in MalNet-Tiny significantly contributes to the brittleness of graph-based malware classifiers under distribution shift. To address this, we propose a comprehensive pipeline for robust malware classification to train a graph classification model for malware samples, as illustrated in Fig. 1. We first reformulate the problem of malware classification as a graph classification task, and present our proposed method for constructing attributed graphs from malware samples. We then discuss data-quality challenges in the original MalNet that hinders the feature extraction process, and how we can mitigate them with our proposed collation schemes.

4.1 Formalizing Robust Feature Extraction

We formally define malware classification as a graph classification task: For each malware sample X , we aim to construct an attributed graph $G = (A, X)$, where $A = \phi_T(X)$ is the adjacency matrix, and $X = \phi_F(X)$ is the node feature matrix¹. This process involves a topology extractor ϕ_T that extracts the graph structure from the malware sample, and a node feature extractor ϕ_F that extracts a feature vector for each vertex in the graph; which we combined as ϕ . The goal is to construct a semantic feature extractor ϕ such that the trained graph classification model \hat{F} performs well on both the training distribution \mathcal{D} and a new testing distribution \mathcal{D}' :

¹For each malware sample, normal X refers to the raw sample, G refers to its graph representation, and bold X refers to the node feature matrix.

PROBLEM 1 (ROBUST FEATURE EXTRACTION FOR GRAPH MALWARE CLASSIFICATION). *Given malware sample X , the goal is to construct an expressive feature extractor $\phi(X)$ that returns the graph representations $G = \phi(X)$, such that the trained model \hat{F} performs well on both the training, i.e. high $\mathbb{P}_{(X,Y)\sim\mathcal{D}}[\hat{F}(G) = Y]$, and new test distribution, i.e. high $\mathbb{P}_{(X,Y)\sim\mathcal{D}'}[\hat{F}(G) = Y]$.*

4.2 Attributed Graph Construction

In this section, we present our proposed method for constructing attributed graphs from malware samples, extending traditional works that only focused on structural features. Specifically, we focus on advanced feature extraction that we believe may aid in mitigating the distribution shift problem. Fig. 1 shows an overview of the feature construction process.

4.2.1 Topology Extractor. We adhere to the original construction of MalNet for topology extraction, utilizing FCGs as the graph representation of malware samples. The FCG contains a node set \mathcal{V} where each node v_i represents a function, and an edge set \mathcal{E} where each edge e_{jk} denotes that function v_j calls function v_k during its execution. Mathematically, we define the topology extractor ϕ_T as a function that takes in a malware sample x and returns the adjacency matrix $\mathbf{A} = \phi_T(X) \in \mathbb{R}^{|\mathcal{V}| \times |\mathcal{V}|}$ of the FCG, where $|\mathcal{V}|$ is the number of nodes/functions, and each entry A_{jk} is 1 if $e_{jk} \in \mathcal{E}$, and 0 otherwise. The resulting graph is then $G = (\mathbf{A}, \emptyset)$, where the node feature matrix is empty.

4.2.2 Feature Extractor. Existing methods [16, 46, 47] typically use Local Degree Profile (LDP) [8] for node feature extraction ϕ_F , which is a vector of the node’s degree and its neighbors’ degree statistics. As LDP focuses solely on the structural properties of the graph, when combined with the purely-structural FCG, it unnecessarily limits the model’s ability to learn from the semantic properties of these function calls, which can be crucial for distinguishing between different types of malwares. Instead, we propose to extract node features directly from the corresponding functions, which better capture the behavior and characteristics of the malwares.

Aggregated Metadata Features. Inspired by EMBER [3], we construct a set of metadata features for each function, which are then aggregated into a single feature vector $\mathbf{x}_{v_i}^{\text{Meta}}$ for each node v_i . Features include *class* and *method names*, *method signatures*, *access flags*, *code length*, *bytecode statistics*, *instruction statistics*, *string statistics*, and *more*. In addition, we extract other Android-specific features such as *storage access*, *registry modifications*, and *in-memory code execution*. This feature construction scheme is designed to capture the essential characteristics of the functions in the FCGs, while not disclosing any sensitive information similar to the EMBER precedence. We refer the reader to Appendix A.2 for detailed specifications.

LLM Source Code Embedding. From the Androguard analysis output, we also obtain the decompiled Java source code of each function, which we use to extract additional features. We utilize CodeXEmbed [38], the only available code embedding model that has a large enough context window to handle the size of the source code, to embed the source code into a numerical vector. The model is pulled from the HuggingFace repository [54], and inference was

done through the provided HuggingFace API. This embedding better extracts the semantic meaning of the function than the aggregated metadata features alone, as it captures the function’s behavior and purpose based on its implementation. We denote the resulting feature vector as $\mathbf{x}_{v_i}^{\text{LLM}}$ for each function v_i . Further details and additional experiments on different LLMs are included in Appendix C.1.

Concatenating Components. While the metadata contains some general properties of a function, incorporating code embeddings generated by LLMs provides a more comprehensive representation of a function’s behavior. This provides additional context for the model to distinguish between functions with similar metadata. This insight leads us to include both types of features in our method. We also utilize the commonly-used LDP features, which were originally employed in previous works [16, 46, 47]:

$$\mathbf{x}_{v_i}^{\text{LDP}} = [\text{deg}(v_i), \min_{v_j \in \mathcal{N}(v_i)} \text{deg}(v_j), \max_{v_j \in \mathcal{N}(v_i)} \text{deg}(v_j), \text{mean}_{v_j \in \mathcal{N}(v_i)} \text{deg}(v_j), \text{std}_{v_j \in \mathcal{N}(v_i)} \text{deg}(v_j)], \quad (1)$$

for any node v_i , where $\text{deg}(v_i)$ is the node degree, and $\mathcal{N}(v_i)$ is the neighborhood of v_i .

The three extracted feature vectors are concatenated to form the final d -dimensional node feature vector:

$$\mathbf{x}_{v_i} = [\mathbf{x}_{v_i}^{\text{Meta}} \quad \mathbf{x}_{v_i}^{\text{LLM}} \quad \mathbf{x}_{v_i}^{\text{LDP}}] \in \mathbb{R}^d,$$

for each node v_i in the FCG. Putting it all together, we define the feature extractor ϕ_F as a function that takes a malware X and its the FCG adjacency matrix \mathbf{A} , and returns the node feature matrix $\mathbf{X} = \phi_F(\mathbf{A}, X) = [\mathbf{x}_{v_1} \dots \mathbf{x}_{v_{|\mathcal{V}|}}]^T \in \mathbb{R}^{|\mathcal{V}| \times d}$, with each row vector \mathbf{x}_{v_i} constructed as described above. As $\mathbf{A} = \phi_T(X)$ can be obtained from the malware sample X and thus can be omitted from the function signature, we henceforth omit it for simplicity. The final attributed graph is then:

$$G = \phi(X) = (\phi_T(X), \phi_F(X)) = (\mathbf{A}, \mathbf{X}). \quad (2)$$

4.3 Handling Data-Quality Challenges

While the topology extractor ϕ_T produces a well-defined graph structure \mathbf{A} for each malware sample, constructing a high-quality node feature matrix $\mathbf{X} = \phi_F(X)$ presents nontrivial data-quality challenges. In particular, the reliability and availability of semantic features extracted from each function in the graph can vary substantially due to limitations in the underlying data. For any given malware sample, the number of extractable semantic features varies from function to function. Some nodes correspond to external or system-level functions (e.g., Android APIs or imported libraries) that lack accessible decompiled source code, making it impossible to compute certain semantic features such as code embeddings. As a result, the feature matrix $\mathbf{X} \in \mathbb{R}^{|\mathcal{V}| \times d}$, where each row $\mathbf{X}_{i,:} \equiv \mathbf{x}_{v_i} \in \mathbb{R}^d$ represents the feature vector for node v_i , is only partially defined, with some node feature entries missing due to limitations in static analysis or obfuscation. To formalize this, we define the set of *non-universal* feature dimensions:

$$C = \{c \in \{1, \dots, d\} \mid \exists i \in \{1, \dots, |\mathcal{V}|\} \text{ s.t. } \mathbf{X}_{i,c} \text{ is missing}\}.$$

These are the feature types that are not consistently available across all nodes in this sample’s graph. However, since the downstream GNN classifier $F(G)$ requires that all nodes in the attributed graph

$G = (\mathbf{A}, \mathbf{X})$ share a consistent input dimension, we must address this structural inconsistency before training. To mitigate this challenge, we propose three node feature collation schemes designed to transform the partially defined \mathbf{X} into a complete, uniform format compatible with GNN-based learning: *Trim*, *Zero*, and *Prune*.

4.3.1 Trim: Remove Non-Universal Feature Dimensions. We remove all feature dimensions that are not available for all nodes in the current sample. That is, we retain only the set of feature dimensions \mathcal{F} that are defined across every node, i.e., $\mathcal{F} = \{1, \dots, d\} \setminus C$. We then construct the trimmed feature matrix as follows:

$$\mathbf{X}_{\text{trim}} = \mathbf{X}_{:, \mathcal{F}} \in \mathbb{R}^{|\mathcal{V}| \times |\mathcal{F}|}.$$

This ensures that every node has a complete and consistent feature vector. However, it discards any partially defined features, potentially removing useful information available for some functions.

4.3.2 Zero: Impute Missing Features with Zeros. We retain the full graph and all feature dimensions, and fill in any missing values with zeros. Let:

$$\mathcal{M} = \{(i, c) \in \{1, \dots, |\mathcal{V}|\} \times C \mid \mathbf{X}_{i,c} \text{ is missing}\}$$

be the index set of node-feature pairs that are undefined. We define the zero-imputed feature matrix $\mathbf{X}_{\text{zero}} \in \mathbb{R}^{|\mathcal{V}| \times d}$ as:

$$\mathbf{X}_{\text{zero}}[i, c] = \begin{cases} \mathbf{X}[i, c] & \text{if } (i, c) \notin \mathcal{M}, \\ 0 & \text{if } (i, c) \in \mathcal{M}. \end{cases}$$

This approach ensures that every node retains a full-length feature vector, enabling direct compatibility with GNN input requirements. It defers to the model to learn whether zeroed features are informative or irrelevant.

4.3.3 Prune: Discard Nodes with Incomplete Feature Vectors. Unlike other strategies which retain the original graph topology, *Prune* modifies both the feature matrix and the graph structure: when a node has missing feature values, we remove it along with any edges connected to it. Formally, we first define the set of nodes with complete feature vectors \mathcal{V}' :

$$\mathcal{V}' = \{v_i \in \mathcal{V} \mid \forall c \in \{1, \dots, d\}, \mathbf{X}_{i,c} \text{ is defined}\}.$$

We then restrict both the feature matrix and the adjacency matrix to this subset. Our newly pruned feature matrix is:

$$\mathbf{X}_{\text{prune}} = \mathbf{X}_{\mathcal{V}', :} \in \mathbb{R}^{|\mathcal{V}'| \times d},$$

and the corresponding pruned graph topology is:

$$\mathbf{A}_{\text{prune}} = \mathbf{A}_{\mathcal{V}', \mathcal{V}'} \in \{0, 1\}^{|\mathcal{V}'| \times |\mathcal{V}'|}.$$

This operation yields the subgraph of G induced by the node set (\mathcal{V}'), thereby ensuring that the input graph provided to the GNN maintains structural consistency and contains fully-defined features. While preserving all feature dimensions, it might omit important contextual information.

5 Graph Learning for Distribution Shifts

After constructing the attributed graph for each malware sample and making sure that all nodes have consistent feature dimensions via one of our proposed collation schemes, we finally leverage powerful GNNs to learn complex malware representations based on our attributed graphs: with each malware transformed into an

attributed graph $G = (\mathbf{A}, \mathbf{X})$, it proceeds to be encoded into a condensed graph-level vector representation via a GNN $F(G)$. Pursuing the goal of building models that remain robust when the test-time data distribution differs from the training, i.e., *distribution shift*, we further improve model generalizability by applying existing model-centric adaptation approaches jointly with our data-centric enrichment scheme. To integrate these model-based techniques into our pipeline, we decompose the learning process into two stages: *upstream training* on the source distribution \mathcal{D} , and *downstream adaptation* to the target distribution \mathcal{D}' .

5.0.1 Upstream Training. In the upstream phase, we assume access to labeled training samples $(G, Y) \sim \mathcal{D}$, where each malware has been converted into an attributed graph. We train a GNN classifier F by minimizing the expected loss:

$$\hat{F} = \arg \min_F \mathbb{E}_{(G, Y) \sim \mathcal{D}} [\mathcal{L}(F(G), Y)]$$

This training step may involve supervised or self-supervised (pre-) training and does not assume any knowledge of \mathcal{D}' .

5.0.2 Downstream Adaptation. At test time, we apply \hat{F} to data drawn from a different distribution \mathcal{D}' , which can result in degraded performance due to distribution shift. To improve generalization, we define a general adaptation framework that produces an adapted model \tilde{F} by modifying \hat{F} using data from \mathcal{D}' , categorized by the target labels' availability.

Test-Time Adaptation (TTA). TTA assumes access to *unlabeled* graphs from the target domain $\{G_j\}_{j=1}^m \sim \mathcal{D}'$, and adapts the model using these samples:

$$\tilde{F} = \mathcal{A}_{\text{TTA}}(\hat{F}; \{G_j\}_{j=1}^m). \quad (3)$$

These methods typically do not modify the entire model but update specific components such as normalization layers or classifier prototypes [31]. TTA is appealing in scenarios where no new annotations are available.

Domain Adaptation (DA). DA assumes access to *labeled* target data $\{(G_k, Y_k)\}_{k=1}^n \sim \mathcal{D}'$ and adapts the model using both graphs and their labels:

$$\tilde{F} = \mathcal{A}_{\text{DA}}(\hat{F}; \{(G_k, Y_k)\}_{k=1}^n). \quad (4)$$

This setting supports stronger forms of adaptation, including full finetuning [11], parameter-efficient updates (e.g., adapters) [21, 24], or classifier replacement [10], although requires additional labeling.

This modular framework cleanly separates the learning process into upstream representation learning and downstream adaptation. It supports a variety of adaptation methods that can be flexibly selected based on real-world constraints such as data availability or deployment cost. In our experiments, we instantiate this framework using both generic and graph-specific methods for TTA and DA.

6 Numerical Evaluation

In this section, we evaluate the performance of current graph-based malware classifiers in the presence of distribution shift on our newly constructed datasets, and investigate the effectiveness of our proposed semantic enrichment framework across different GNN architectures and adaptation methods. For the latter goal, we pose a series of research questions for a thorough evaluation:

RQ1: How do semantic features affect model robustness?

We address this question by comparing models trained with and without semantic features on the original dataset, evaluated on the same testing distribution (i.e. high utility), and on a covariate-shifted testing distribution (i.e. high robustness).

RQ2: Are all features necessary for improving robustness?

We conduct an ablation study on the two components of our semantic feature construction across different collation schemes, and report how they affect model performance.

RQ3: Do features work with existing adaptation methods?

Given that our method takes a different approach to alleviating distribution shift, we evaluate how well it can be combined with and improve existing adaptation methods.

We design and conduct a series of experiments to answer these questions, giving insights into the characteristics of semantic features for malware FCGs, and report our findings.

6.1 Experimental Setup

Below, we concisely outline our experiment configurations. A more detailed description can be found in Appendix B.

GNN Architectures. Depending on the model architecture, different feature collation schemes may be better or worse. Therefore, we conduct our experiments with various GNN architectures, including GCN [35], GIN [56], GPS [46], and Exphormer [47].

Adaptation Methods. We select these methods such that they do not alter the upstream training process, and cover a wide range of approaches. For Test-time Adaptation (TTA), the selected baselines are Tent [50], T3A [31], and GTrans [32]. For Domain Adaptation (DA) approaches, we evaluate with k-NN Probe [10], normal fine-tuning, and AdapterGNN [37].

6.2 Results & Findings

6.2.1 Standard Training Under Covariate Shift. Tab. 2 shows the results of our experiments on the original MalNet-Tiny and its covariate-shifted counterpart MalNet-Tiny-Common. With no semantic features, for all GNN architectures, accuracy drops by almost half when evaluated on the shifted distribution, up to a difference of 45.3% in the case of GPS. This confirms the severity of distribution shift in real-world malware classification tasks, and motivates the need for robust models that can generalize well to unseen data. We next investigate how our proposed semantic feature construction affects model robustness.

RQ1: How do semantic features affect model robustness?

We observe that every models trained with semantic features outperform when compared to the baselines trained without.

FINDING 1. *Prune achieves the highest accuracy for traditional message-passing architectures (MPNNs), while Zero achieves the highest accuracy for Transformer-based ones.*

As *Trim* achieves a lower accuracy for most cases, we can confirm that our feature construction scheme benefits the graph models’ performance. The lower results of *Zero* on traditional MPNNs tells us that these primitive architectures are misguided by the missing features; whereas the more modern graph transformers are robust to the absence of information, resulting in a better utilization of these

Tab. 2: Test accuracy on MalNet-Tiny and MalNet-Tiny-Common with/without semantic features. Highest values are bolded.

Method	GCN		GIN		GPS		Exphormer	
	Tiny	Cmn.	Tiny	Cmn.	Tiny	Cmn.	Tiny	Cmn.
Baseline	85.7%	48.1%	90.4%	47.4%	93.5%	48.2%	93.3%	48.4%
Trim	91.5%	55.2%	92.2%	51.7%	94.3%	56.9%	95.0%	56.4%
Prune	95.2%	60.3%	94.8%	61.6%	94.9%	56.7%	95.0%	55.3%
Zero	94.6%	59.0%	94.9%	59.1%	95.3%	56.7%	95.0%	57.0%

partially-available features. These findings are further corroborated by a more comprehensive set of experiments below.

RQ2: Are all features necessary for improving model robustness?

To further delve into the contribution of each of our components, we conduct an ablation study on the feature configurations. We select the commonly-used LDP features as our baseline, experiment with replacing or adding features, and measure the resulting differences. Note that *Trim* does not work with LLM features: for all Android packages, there exist some functions that do not have any code in the APK (e.g. API functions). As a result, code embedding is not a universal feature, and thus will always be trimmed. Tab. 3 presents the full results of our ablation study.

FINDING 2. *For any feature and collation configurations, all models achieved higher results than the baseline.*

This strengthens our claim of effectiveness for semantic features with these two collation schemes. As different GNNs response differently to each pipeline configuration, a practitioner may use these results to select an appropriate set of hyperparameters for their specific use cases. We discuss this topic in Sec. 7.1, and provide further quantitative justification in Appendix C.

FINDING 3. *Transformer-based architectures achieve a higher in-distribution accuracy than MPNNs, but performs worse on distribution-shifted data.*

During training, the models learn from the training distribution, and their final checkpoints are selected based on the corresponding validation set. This naturally results in these models fitting as much as possible to said distribution, as the early-stopping only prevents overfitting to the training *set*, not the distribution itself. Given that the Transformer models have a higher discriminative power than MPNNs, they learned to work better on the trained task in exchange for a comparatively lower performance on covariate-shifted data.

FINDING 4. *With adequate semantic context, simple MPNNs can achieve near the performance of Transformer-based architectures, while performing better under distribution shift.*

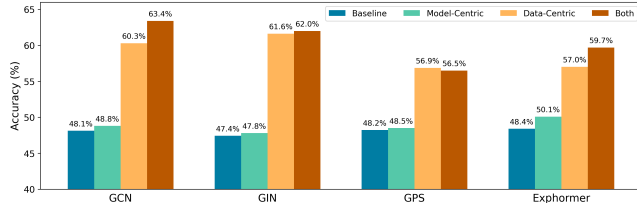
For upstream classification, this phenomenon is best shown where GCN, a basic architecture, achieved 9.5% improvement in upstream task, outperforming the best Exphormer result. Similarly, GIN, a discriminative-oriented MPNN, increased its distribution-shifted accuracy by 14.2%, far higher than the Transformer-based counterparts. These results show that the inherent lower representation capacity of primitive architectures can be more than compensated with good feature constructions for the input graph. Additionally, we can conclude that our pipeline not only improves the models’ general prediction capacity, but also their robustness. This is evident by the much larger gain in downstream accuracy comparing to which evaluated on the upstream distribution.

Tab. 3: Models’ accuracy on MalNet-Tiny and MalNet-Tiny-Common across different feature configurations. Top 5 highest values are highlighted in green, darker green represents higher accuracy. Subscript denotes standard deviation over 3 independent runs.

Method	Features			GCN		GIN		GPS		Expformer	
	Meta	LLM	LDP	Tiny	Cmn.	Tiny	Cmn.	Tiny	Cmn.	Tiny	Cmn.
Baseline / None			✓	85.67 _{0.58}	48.13 _{0.26}	90.40 _{1.44}	47.43 _{0.48}	93.53 _{0.09}	48.23 _{0.29}	93.27 _{0.49}	48.40 _{0.24}
Trim	✓	-	-	91.47 _{0.39}	55.20 _{0.99}	91.13 _{0.66}	51.67 _{0.53}	94.30 _{0.16}	52.90 _{0.78}	94.50 _{0.45}	56.43 _{2.24}
	✓	-	✓	91.53 _{0.40}	51.07 _{0.45}	92.20 _{0.24}	51.73 _{1.00}	94.33 _{0.69}	56.87_{2.03}	95.00_{0.22}	51.57 _{1.32}
Prune	✓	-	-	93.33 _{0.09}	54.40 _{0.50}	92.73 _{0.70}	55.17 _{1.25}	93.63 _{0.26}	54.47 _{1.16}	94.40 _{0.37}	51.73 _{1.31}
	✓	-	✓	92.87 _{0.39}	51.30 _{1.70}	93.47 _{0.54}	54.60 _{0.71}	94.27 _{0.77}	54.37 _{1.28}	94.30 _{0.70}	54.70 _{2.07}
	-	✓	-	94.33 _{0.24}	60.30_{1.98}	94.30 _{0.43}	61.10_{0.22}	94.77 _{0.26}	53.50 _{2.12}	94.50 _{0.22}	55.27 _{0.66}
	-	✓	✓	94.33 _{0.29}	58.33 _{1.72}	94.83 _{0.42}	59.97 _{0.95}	94.80 _{0.28}	53.07 _{0.73}	94.97 _{0.52}	54.87 _{1.52}
	✓	✓	-	95.17_{0.33}	59.70 _{0.41}	94.20 _{0.24}	61.63_{2.19}	94.87 _{0.41}	55.57 _{1.52}	95.00_{0.43}	52.37 _{0.12}
Zero	✓	-	-	93.60 _{0.37}	54.27 _{0.79}	93.30 _{0.73}	52.83 _{0.74}	94.37 _{0.25}	54.90 _{1.41}	93.67 _{0.29}	53.50 _{2.94}
	✓	-	✓	92.57 _{0.26}	50.20 _{0.99}	93.67 _{0.34}	53.40 _{1.28}	94.20 _{0.36}	50.87 _{0.87}	94.00 _{0.51}	57.03_{0.46}
	-	✓	-	94.60 _{0.22}	56.70 _{2.03}	94.27 _{0.26}	58.60 _{1.70}	95.10_{0.36}	56.73_{0.54}	94.60 _{0.43}	55.57 _{1.58}
	-	✓	✓	94.57 _{0.41}	58.60 _{1.19}	94.50 _{0.36}	56.57 _{0.34}	94.60 _{0.37}	54.87 _{1.39}	95.00_{0.22}	55.33 _{2.33}
	✓	✓	-	93.80 _{0.16}	58.87 _{1.46}	94.93_{0.34}	56.33 _{0.62}	95.27_{0.21}	54.97 _{1.48}	94.97 _{0.47}	55.87 _{0.31}
✓	✓	✓	94.37 _{0.37}	59.00 _{0.86}	94.93_{0.29}	59.10 _{0.67}	94.53 _{0.09}	53.60 _{0.67}	94.40 _{0.08}	54.73 _{1.43}	

Tab. 4: Accuracy on MalNet-Tiny-Common when combining TTA methods with semantic features. Highest values for each set are in bold. XFM is short for Expformer.

Model	GCN	GIN	GPS	XFM
Tent	44.90%	47.80%	47.90%	46.60%
... + Prune	61.70%	60.70%	52.00%	52.20%
... + Zero	58.50%	56.20%	53.80%	55.70%
T3A	48.80%	46.80%	48.50%	47.90%
... + Prune	63.40%	62.00%	52.00%	55.60%
... + Zero	59.50%	57.70%	56.50%	56.50%
GTrans	47.50%	47.20%	48.50%	50.10%
... + Prune	62.00%	61.40%	55.00%	56.50%
... + Zero	58.90%	57.70%	54.40%	59.70%

**Fig. 3: Models’ accuracy under covariate shift after applying model-centric adaptation and/or data-centric augmentation.**

6.2.2 Adaptation-Based Training for Distribution Shift. We plot the best accuracy achieved for different GNNs using existing model-centric approaches and our data-centric augmentation when evaluating on MalNet-Tiny-Common in Fig. 3. Our feature construction method consistently beats TTA methods on their own, and in all cases but one architecture further improve OOD performance when used in conjunction with TTA methods.

For a more in-depth analysis of the complementary effect of these two paradigms, we then evaluate the out-of-distribution performance of different GNNs when combined with each TTA method. Tab. 4 reports the results of our experiments, which show that most test-time approaches do not help generalizing to these new variants.

RQ3: Do semantic features work with existing adaptation methods?

Tab. 5: Full dataset accuracy on MalNet-Tiny variants (Common, Distinct) of models trained on MalNet-Tiny after finetuning. Largest accuracy for each experiment set is in bold.

Method	GCN		GIN		GPS		Expformer	
	Cmn.	Dst.	Cmn.	Dst.	Cmn.	Dst.	Cmn.	Dst.
Finetune	81.4%	94.8%	86.4%	96.3%	92.7%	97.2%	93.3%	97.8%
... + Prune	96.8%	96.8%	94.7%	97.2%	96.9%	98.7%	97.1%	97.8%
... + Zero	96.0%	97.2%	94.7%	97.3%	97.0%	98.4%	96.8%	97.9%
k-NN Probe	75.1%	90.3%	75.0%	87.4%	71.0%	87.5%	71.6%	87.5%
... + Prune	85.7%	86.3%	80.1%	85.7%	78.8%	89.2%	76.4%	90.4%
... + Zero	84.2%	89.8%	80.7%	84.5%	78.9%	90.5%	79.5%	89.6%
AdapterGNN	80.2%	94.9%	83.8%	95.7%	87.3%	95.6%	87.1%	96.9%
... + Prune	91.8%	95.3%	87.2%	91.1%	93.7%	96.6%	92.8%	96.2%
... + Zero	90.7%	95.1%	86.9%	91.8%	92.4%	95.8%	91.2%	96.5%

FINDING 5. Our method consistently improves the performance of the adapted models across different generic TTA methods and architectures. Specifically, Prune works best with MPNNs while Zero works best with Transformers.

Besides a higher accuracy across all experiments, we note that our previous findings on the effects of architectural differences are consistent in the TTA scenario. Specifically, Prune continues to work best on MPNNs, delivering higher covariate-shifted results when compared to Transformers, which are more suitable to the Zero collation scheme.

Finetuning-based adaptation. To better improve performance under severe distribution shifts, some methods opt for adapting the model weights directly assuming the availability of additional labeled OOD data. While this requirement is unrealistic in mitigating zero-day attacks, it can be applicable in the case of a post-hoc update to an existing detector. In this more lax setting, all DA methods reach near the standard finetuning baseline (c.f. Tab. 5).

FINDING 6. Our method consistently further improves the adapted models across different finetuning approaches.

The performance on the covariate-shifted dataset still consistently increase by up to 15.4% on GCN, rivaling modern architectures in all cases. This observation confirms the intuition that

simpler models that fit less closely to the training distribution can be more easily adapted to a new downstream task. On the contrary, the only exception arises when evaluating on the domain-shifted dataset, where DA methods sometimes work better without our semantic features. With low/no tunable parameters, these approaches become less capable the handle the more information we provide the model. In practice however, any distribution update is applied using low-epoch finetuning, in which our pipeline always provide superior results comparing to all other settings.

7 Discussions

7.1 Practical Applicability

The empirical results presented in Sec. 6.2 provide a clear decision-making framework for deploying robust malware detection systems. We concisely identify three key dimensions for practical implementation, and present numerical justifications later in Appendix C.

7.1.1 Model Selection: Speed vs. Utility vs. Robustness. As different configurations behave differently under the same data distribution, with the results from our ablation studies (c.f. Tab. 3), one can make a calculated decision when considering the tradeoffs for their specific needs. We provide here some general guidelines as suggestions:

- For resource constraints, we recommend using *GIN-Prune* with only metafeatures. GIN is the smallest and fastest architecture, and we have negligible computation overhead: the time needed to process metafeatures is heavily dominated by the time needed to deconstruct the APK, which is required during FCG extraction. If LLM features are desired for a more balanced tradeoff, smaller LLMs can be used—refer to Appendix C.1 for the ablation studies.
- For peak utility, *GPS-Zero* with only semantic features (i.e. no LDP) yield the highest in-distribution test accuracy. However, note that GPS is very slow – roughly 10.3 times slower than GIN.
- For maximum robustness, *GIN-Prune* with only semantic features performed the best under covariate shift, trading off only 1% from the optimal upstream accuracy for a 6.67% gain under OOD.

7.1.2 Continuous Adaptation to New Threats. Continuous updates have been the proper practice against the rapid evolvement of malwares, with antiviruses frequently updating their definition databases. Equivalently for the ML-powered counterpart, the classifier’s weights should also be frequently updated whenever new malware variants are discovered, given that domain adaptation improved the most for out-of-distribution performance (c.f. Tab. 5). While DA approaches can be costly in terms of computation, it can be justified by amortizing by the large number of benefiting end users. Additionally, in this scenario, Exphormer should be the preferred choice of architecture if accuracy is of utmost importance.

7.1.3 Handling Low-Quality Data Samples. In real-world deployment, malware binaries are often obfuscated or rely heavily on external system libraries that lack source code for LLM embedding. Our framework’s ability to handle partially-defined graphs (Sec. 4.3) ensures that the system does not fail when features are missing. A final note, in scenarios where the malware is fully composed of externally-compiled functions (and thus decompilation is impossible), we suggest opting for metafeature-only configuration to not dilute the model’s attention to these unavailable features.

7.2 Ethics Statement

7.2.1 Data Privacy & Consent. The data source used in this work are readily-available applications on AndroZoo [2], collected and derived with explicit permission of the original maintainer. All samples were pre-processed to remove any Personally Identifiable Information and raw executable code [3]. Our release contains only extracted features representing the software’s control flow and the general semantic properties of the functions, ensuring that no sensitive user data or proprietary source code is exposed. The representations are benign and cannot be executed to perform malicious actions. Labeling is provided by MalNet [16] with a CC-BY license, permitting modification to the data with proper attribution.

7.2.2 Bias. We acknowledge inherent biases in the source from which we curated our datasets: temporally, MalNet does not reflect the real-world distribution of malware in 2026. The dataset comprises older samples (typically pre-2021), potentially under-representing modern evasion techniques. Additionally, the specific choice of repository sources may skew the data toward popular mainstream families (as evident in the adware-related labelings), and overlook more severe 0-day exploits in the black market.

7.2.3 Potential Misuse. While this research aims to improve defense mechanisms, the techniques developed for analyzing graph structures could theoretically be used by adversaries to:

- (1) **Adversarial Evasion:** Analyze feature importance to craft malware that minimizes detection probability.
- (2) **Malware Reconstruction:** Reverse-engineer the graph representations to reconstruct the original malware.
- (3) **Obfuscation:** Understand which structural patterns trigger classifiers to better hide malicious logic.

However, the first threat requires a significant amount of further research, as translating perturbations in the feature space back to the sample space in a valid manner is a nontrivial open problem in automated malware construction [43]. The second threat is heavily mitigated as we have stripped off all identifiable information from the released dataset per standard practices [3]. The third one is rather a necessary evil, as we believe the benefit of hardening defenses against these threats outweighs the risk, as defensive transparency is necessary for robust security – otherwise, we would fall into the trap of *security through obscurity*.

8 Conclusion

In this work, we introduced two new datasets, MalNet-Tiny-Common and MalNet-Tiny-Distinct, to evaluate the robustness of Android malware classifiers against covariate and domain shifts, respectively. Additionally, we constructed a semantic enrichment framework for Android function call graphs using function metadata and LLM-based code embeddings, demonstrating the effectiveness of our data-centric methodology in improving resilience of graph-based classifiers under distribution shift while maintaining strong performance on standard evaluation splits, which can be used in conjunction with existing model-based adaptation methods. We hope this work will enable further research on enriching input graphs to improve the generalization of malware detectors and stimulate future works on semantics-aware graph representations for evolving threat environments.

References

- [1] Hisham Alasmary, Aminollah Khormali, Afsah Anwar, Jeman Park, Jinchun Choi, Ahmed Abusnaina, Amro Awad, Daehun Nyang, and Aziz Mohaisen. 2019. Analyzing and Detecting Emerging Internet of Things Malware: A Graph-Based Approach. *IEEE Internet of Things Journal* 6, 5 (2019), 8977–8988. doi:10.1109/JIOT.2019.2925929
- [2] Kevin Allix, Tegawendé F. Bissyandé, Jacques Klein, and Yves Le Traon. 2016. AndroZoo: Collecting Millions of Android Apps for the Research Community. In *Proceedings of the 13th International Conference on Mining Software Repositories (Austin, Texas) (MSR '16)*. ACM, New York, NY, USA, 468–471. doi:10.1145/2901739.2903508
- [3] Hyrum S. Anderson and Phil Roth. 2018. EMBER: An Open Dataset for Training Static PE Malware Machine Learning Models. arXiv:1804.04637 [cs.CR] <https://arxiv.org/abs/1804.04637>
- [4] Daniel Arp, Michael Spreitzerbarth, Malte Hubner, Hugo Gascon, Konrad Rieck, and CERT Siemens. 2014. Drebin: Effective and explainable detection of android malware in your pocket.. In *Ndss*, Vol. 14. 23–26.
- [5] Wenxuan Bao, Zhichen Zeng, Zhining Liu, Hanghang Tong, and Jingrui He. 2024. Matcha: Mitigating Graph Structure Shifts with Test-Time Adaptation. *arXiv preprint arXiv:2410.06976* (2024).
- [6] Parthajit Borah, DK Bhattacharyya, and JK Kalita. 2020. Malware Dataset Generation and Evaluation. In *2020 IEEE 4th Conference on Information & Communication Technology (CICT)*. IEEE, 1–6.
- [7] Hendrio Bragança, Diego Kreutz, Vanderson Rocha, Joner Assolin, and Eduardo Feitosa. 2025. MH-1M: A 1.34 Million-Sample Multi-Feature Android Malware Dataset with Rich Metadata. *Scientific Data* (2025).
- [8] Chen Cai and Yusu Wang. 2022. A simple yet effective baseline for non-attributed graph classification. arXiv:1811.03508 [cs.LG] <https://arxiv.org/abs/1811.03508>
- [9] Guanzi Chen, Jiyang Zhang, Xi Xiao, and Yang Li. 2022. GraphTTA: Test Time Adaptation on Graph Neural Networks. arXiv:2208.09126 [cs.LG] <https://arxiv.org/abs/2208.09126>
- [10] Ting Chen, Simon Kornblith, Mohammad Norouzi, and Geoffrey Hinton. 2020. A Simple Framework for Contrastive Learning of Visual Representations. arXiv:2002.05709 [cs.LG] <https://arxiv.org/abs/2002.05709>
- [11] Kenneth Ward Church, Zeyu Chen, and Yanjun Ma. 2021. Emerging trends: A gentle introduction to fine-tuning. *Natural Language Engineering* 27, 6 (2021), 763–778.
- [12] Anthony Desnos and Geoffroy Gueguen. 2018. Androguard documentation. *Obtenido de Androguard* (2018).
- [13] Taoran Fang, Yunchao Zhang, Yang Yang, Chunping Wang, and Lei Chen. 2024. Universal Prompt Tuning for Graph Neural Networks. arXiv:2209.15240 [cs.LG] <https://arxiv.org/abs/2209.15240>
- [14] Pengbin Feng, Jianfeng Ma, Teng Li, Xindi Ma, Ning Xi, and Di Lu. 2021. Android Malware Detection via Graph Representation Learning. *Mobile Information Systems* 2021 (2021), 1–14. doi:10.1155/2021/5538841
- [15] Pengbin Feng, Li Yang, Di Lu, Ning Xi, and Jianfeng Ma. 2023. BejaGNN: behavior-based Java malware detection via graph neural network. *The Journal of Supercomputing* 79, 14 (2023), 15390–15414.
- [16] Scott Freitas, Yuxiao Dong, Joshua Neil, and Duen Horng Chau. 2021. A Large-Scale Database for Graph Representation Learning. arXiv:2011.07682 [cs.LG] <https://arxiv.org/abs/2011.07682>
- [17] Scott Freitas, Rahul Duggal, and Duen Horng Chau. 2022. MalNet: A Large-Scale Image Database of Malicious Software. arXiv:2102.01072 [cs.CR] <https://arxiv.org/abs/2102.01072>
- [18] Xingbo Fu, Yinhan He, and Jundong Li. 2025. Edge Prompt Tuning for Graph Neural Networks. arXiv:2503.00750 [cs.LG] <https://arxiv.org/abs/2503.00750>
- [19] Xiuting Ge, Ya Pan, Yong Fan, and Chunrong Fang. 2019. AMDroid: Android Malware Detection Using Function Call Graphs. In *2019 IEEE 19th International Conference on Software Quality, Reliability and Security Companion (QRS-C)*. 71–77. doi:10.1109/QRS-C.2019.00027
- [20] Alejandro Guerra-Manzanares, Hayretin Bahsi, and Sven Nömm. 2021. KronoDroid: Time-based Hybrid-featured Dataset for Effective Android Malware Detection and Characterization. *Computers & Security* 110 (2021), 102399. doi:10.1016/j.cose.2021.102399
- [21] Anchun Gui, Jinqiang Ye, and Han Xiao. 2023. G-Adapter: Towards Structure-Aware Parameter-Efficient Transfer Learning for Graph Transformer Networks. arXiv:2305.10329 [cs.LG] <https://arxiv.org/abs/2305.10329>
- [22] Daya Guo, Shuai Lu, Nan Duan, Yanlin Wang, Ming Zhou, and Jian Yin. 2022. UniXcoder: Unified Cross-Modal Pre-training for Code Representation. arXiv:2203.03850 [cs.CL] <https://arxiv.org/abs/2203.03850>
- [23] William L. Hamilton, Rex Ying, and Jure Leskovec. 2018. Inductive Representation Learning on Large Graphs. arXiv:1706.02216 [cs.SI] <https://arxiv.org/abs/1706.02216>
- [24] Zeyu Han, Chao Gao, Jinyang Liu, Jeff Zhang, and Sai Qian Zhang. 2024. Parameter-Efficient Fine-Tuning for Large Models: A Comprehensive Survey. arXiv:2403.14608 [cs.LG] <https://arxiv.org/abs/2403.14608>
- [25] Md Ahsanul Haque, Ismail Hossain, Md Mahmuduzzaman Kamol, Md Jahangir Alam, Suresh Kumar Amalapuram, Sajedul Talukder, and Mohammad Saidur Rahman. 2025. LAMDA: A Longitudinal Android Malware Benchmark for Concept Drift Analysis. arXiv:2505.18551 [cs.CR] <https://arxiv.org/abs/2505.18551>
- [26] Richard Harang and Ethan M. Rudd. 2020. SOREL-20M: A Large Scale Benchmark Dataset for Malicious PE Detection. arXiv:2012.07634 [cs.CR] <https://arxiv.org/abs/2012.07634>
- [27] Shifu Hou, Yujie Fan, Yiming Zhang, Yanfang Ye, Jingwei Lei, Wenqiang Wan, Jiabin Wang, Qi Xiong, and Fudong Shao. 2019. aCyber: Enhancing Robustness of Android Malware Detection System against Adversarial Attacks on Heterogeneous Graph based Model. In *Proceedings of the 28th ACM International Conference on Information and Knowledge Management (Beijing, China) (CIKM '19)*. Association for Computing Machinery, New York, NY, USA, 609–618. doi:10.1145/3357384.3357875
- [28] Hans Hao-Hsun Hsu, Shikun Liu, Han Zhao, and Pan Li. 2025. Structural Alignment Improves Graph Test-Time Adaptation. arXiv:2502.18334 [cs.LG] <https://arxiv.org/abs/2502.18334>
- [29] Weihua Hu, Matthias Fey, Marinka Zitnik, Yuxiao Dong, Hongyu Ren, Bowen Liu, Michele Catasta, and Jure Leskovec. 2020. Open Graph Benchmark: Datasets for Machine Learning on Graphs. *arXiv preprint arXiv:2005.00687* (2020).
- [30] Médéric Hurier. 2025. Euphony. <https://github.com/fmind/euphony>.
- [31] Yusuke Iwasawa and Yutaka Matsuo. 2021. Test-Time Classifier Adjustment Module for Model-Agnostic Domain Generalization. In *Advances in Neural Information Processing Systems*, M. Ranzato, A. Beygelzimer, Y. Dauphin, P.S. Liang, and J. Wortman Vaughan (Eds.), Vol. 34. Curran Associates, Inc., 2427–2440. https://proceedings.neurips.cc/paper_files/paper/2021/file/1415fe9ea0fa1e45dddcff5682239a0-Paper.pdf
- [32] Wei Jin, Tong Zhao, Jiayuan Ding, Yozen Liu, Jiliang Tang, and Neil Shah. 2023. Empowering Graph Representation Learning with Test-Time Graph Transformation. In *The Eleventh International Conference on Learning Representations*. <https://openreview.net/forum?id=Lnx5pr018>
- [33] Robert J. Joyce, Dev Amlani, Charles Nicholas, and Edward Raff. 2021. MO-TIF: A Large Malware Reference Dataset with Ground Truth Family Labels. arXiv:2111.15031 [cs.LG] <https://arxiv.org/abs/2111.15031>
- [34] Mingxuan Ju, Tong Zhao, Wenhao Yu, Neil Shah, and Yanfang Ye. 2023. Graph-Patcher: Mitigating Degree Bias for Graph Neural Networks via Test-time Augmentation. arXiv:2310.00800 [cs.LG] <https://arxiv.org/abs/2310.00800>
- [35] Thomas N. Kipf and Max Welling. 2017. Semi-Supervised Classification with Graph Convolutional Networks. arXiv:1609.02907 [cs.LG] <https://arxiv.org/abs/1609.02907>
- [36] Ce Li, Zijun Cheng, He Zhu, Leiqi Wang, Qiujian Lv, Yan Wang, Ning Li, and Degang Sun. 2022. DMalNet: Dynamic malware analysis based on API feature engineering and graph learning. *Computers & Security* 122 (2022), 102872. doi:10.1016/j.cose.2022.102872
- [37] Shengrui Li, Xueting Han, and Jing Bai. 2023. AdapterGNN: Parameter-Efficient Fine-Tuning Improves Generalization in GNNs. arXiv:2304.09595 [cs.LG] <https://arxiv.org/abs/2304.09595>
- [38] Ye Liu, Rui Meng, Shafiq Joty, Silvio Savarese, Caiming Xiong, Yingbo Zhou, and Semih Yavuz. 2024. CodeXEmbed: A Generalist Embedding Model Family for Multilingual and Multi-task Code Retrieval. arXiv:2411.12644 [cs.SE] <https://arxiv.org/abs/2411.12644>
- [39] Zemin Liu, Xingtong Yu, Yuan Fang, and Xinming Zhang. 2023. GraphPrompt: Unifying Pre-Training and Downstream Tasks for Graph Neural Networks. arXiv:2302.08043 [cs.LG] <https://arxiv.org/abs/2302.08043>
- [40] Samaneh MahdaviFar, Dima Alhadidi, and Ali A Ghorbani. 2022. Effective and efficient hybrid android malware classification using pseudo-label stacked auto-encoder. *Journal of network and systems management* 30, 1 (2022), 22.
- [41] Saleh J. Makkawy, Michael J. De Lucia, and Kenneth E. Barner. 2025. MalVis: A Large-Scale Image-Based Framework and Dataset for Advancing Android Malware Classification. arXiv:2505.12106 [cs.CR] <https://arxiv.org/abs/2505.12106>
- [42] Tomas Mikolov, Kai Chen, Greg Corrado, and Jeffrey Dean. 2013. Efficient Estimation of Word Representations in Vector Space. arXiv:1301.3781 [cs.CL] <https://arxiv.org/abs/1301.3781>
- [43] Fabio Pierazzi, Feargus Pendlebury, Jacopo Cortellazzi, and Lorenzo Cavallaro. 2020. Intriguing properties of adversarial ml attacks in the problem space. In *2020 IEEE symposium on security and privacy (SP)*. IEEE, 1332–1349.
- [44] Nikhil Prakash, Tamar Rott Shaham, Tal Haklay, Yonatan Belinkov, and David Bau. 2024. Fine-Tuning Enhances Existing Mechanisms: A Case Study on Entity Tracking. arXiv:2402.14811 [cs.CL] <https://arxiv.org/abs/2402.14811>
- [45] Joaquin Quiñero-Candela, Masashi Sugiyama, Anton Schwaighofer, and Neil D Lawrence. 2022. *Dataset shift in machine learning*. Mit Press.
- [46] Ladislav Rampásek, Mikhail Galkin, Vijay Prakash Dwivedi, Anh Tuan Luu, Guy Wolf, and Dominique Beaini. 2023. Recipe for a General, Powerful, Scalable Graph Transformer. arXiv:2205.12454 [cs.LG] <https://arxiv.org/abs/2205.12454>
- [47] Hamed Shirzad, Ameya Velingker, Balaji Venkatachalam, Danica J. Sutherland, and Ali Kemal Sinop. 2023. Exphormer: Sparse Transformers for Graphs. arXiv:2303.06147 [cs.LG] <https://arxiv.org/abs/2303.06147>

- [48] Gaurav Sood. 2021. *virustotal: R Client for the virustotal API*.
- [49] Xiangguo Sun, Hong Cheng, Jia Li, Bo Liu, and Jihong Guan. 2023. All in One: Multi-task Prompting for Graph Neural Networks. arXiv:2307.01504 [cs.SI] <https://arxiv.org/abs/2307.01504>
- [50] Dequan Wang, Evan Shelhamer, Shaoteng Liu, Bruno Olshausen, and Trevor Darrell. 2021. Tent: Fully Test-time Adaptation by Entropy Minimization. arXiv:2006.10726 [cs.LG] <https://arxiv.org/abs/2006.10726>
- [51] Yiqi Wang, Chaozhuo Li, Wei Jin, Rui Li, Jianan Zhao, Jiliang Tang, and Xing Xie. 2022. Test-Time Training for Graph Neural Networks. arXiv:2210.08813 [cs.LG] <https://arxiv.org/abs/2210.08813>
- [52] Kilian Weinberger, Anirban Dasgupta, John Langford, Alex Smola, and Josh Attenberg. 2009. Feature hashing for large scale multitask learning. In *Proceedings of the 26th annual international conference on machine learning*. 1113–1120.
- [53] Boris Weisfeiler and Andrei Leman. 1968. The reduction of a graph to canonical form and the algebra which appears therein. *nti, Series 2*, 9 (1968), 12–16.
- [54] Thomas Wolf, Lysandre Debut, Victor Sanh, Julien Chaumond, Clement Delangue, Anthony Moi, Pierric Cistac, Tim Rault, Rémi Louf, Morgan Funtowicz, Joe Davison, Sam Shleifer, Patrick von Platen, Clara Ma, Yacine Jernite, Julien Plu, Canwen Xu, Teven Le Scao, Sylvain Gugger, Mariama Drame, Quentin Lhoest, and Alexander M. Rush. 2020. HuggingFace’s Transformers: State-of-the-art Natural Language Processing. arXiv:1910.03771 [cs.CL] <https://arxiv.org/abs/1910.03771>
- [55] Man Wu, Xin Zheng, Qin Zhang, Xiao Shen, Xiong Luo, Xingquan Zhu, and Shirui Pan. 2024. Graph learning under distribution shifts: A comprehensive survey on domain adaptation, out-of-distribution, and continual learning. *arXiv preprint arXiv:2402.16374* (2024).
- [56] Keyulu Xu, Weihua Hu, Jure Leskovec, and Stefanie Jegelka. 2019. How Powerful are Graph Neural Networks? arXiv:1810.00826 [cs.LG] <https://arxiv.org/abs/1810.00826>
- [57] An Yang, Anfeng Li, Baosong Yang, Beichen Zhang, Binyuan Hui, Bo Zheng, Bowen Yu, Chang Gao, Chengen Huang, Chenxu Lv, Chujie Zheng, Dayiheng Liu, Fan Zhou, Fei Huang, Feng Hu, Hao Ge, Haoran Wei, Huan Lin, Jialong Tang, Jian Yang, Jianhong Tu, Jianwei Zhang, Jianxin Yang, Jiayi Yang, Jing Zhou, Jingren Zhou, Junyang Lin, Kai Dang, Keqin Bao, Kexin Yang, Le Yu, Lianhao Deng, Mei Li, Mingfeng Xue, Mingze Li, Pei Zhang, Peng Wang, Qin Zhu, Rui Men, Ruize Gao, Shixuan Liu, Shuang Luo, Tianhao Li, Tianyi Tang, Wenbiao Yin, Xingzhang Ren, Xinyu Wang, Xinyu Zhang, Xuancheng Ren, Yang Fan, Yang Su, Yichang Zhang, Yinger Zhang, Yu Wan, Yuqiong Liu, Zekun Wang, Zeyu Cui, Zhenru Zhang, Zhipeng Zhou, and Zihan Qiu. 2025. Qwen3 Technical Report. arXiv:2505.09388 [cs.CL] <https://arxiv.org/abs/2505.09388>
- [58] Limin Yang, Arridhana Ciptadi, Ihar Laziuk, Ali Ahmadzadeh, and Gang Wang. 2021. BODMAS: An Open Dataset for Learning based Temporal Analysis of PE Malware. In *4th Deep Learning and Security Workshop*.
- [59] Chunyan Zhang, Qinglei Zhou, Yizhao Huang, Ke Tang, Hairan Gui, and Fudong Liu. 2022. Automatic Detection of Android Malware via Hybrid Graph Neural Network. *Wireless Communications and Mobile Computing 2022*, 1 (2022), 7245403. arXiv:<https://onlinelibrary.wiley.com/doi/pdf/10.1155/2022/7245403> doi:10.1155/2022/7245403
- [60] Yajin Zhou and Xuxian Jiang. 2012. Dissecting android malware: Characterization and evolution. In *2012 IEEE symposium on security and privacy*. IEEE, 95–109.

A Dataset Construction Specifications

A.1 Original MalNet Construction.

Collected from AndroZoo [2], each malware sample in MalNet [16] is represented by its function call graph (FCG). These FCGs are generated using AndroGuard [12], with any other extracted information discarded during the process. The corresponding malware labels were collected from VirusTotal [48], a service detecting malicious files by providing their analysis reports from antivirus (AV) engines. These reports categorize malwares into their *families* and *types* based on their behavior and characteristics, and are unified into one final label for the dataset using Euphony [30]. An structure example of this hierarchical labeling is shown in Fig. 4. As detection results of different AVs do not always agree, the unified labels can be very noisy, which can lead to ambiguity in classification tasks. To address this, the authors of MalNet introduced the *MalNet-Tiny* subset, which is a smaller version of the original dataset with balanced sample distribution across different classes, where each class contains exactly one malware family and one malware type

classification. This subset is designed to be more manageable for training and evaluation purposes, while still retaining the essential characteristics of the original dataset.

A.2 MalNet Function Metafeature Specifications

We construct function node metafeatures by adapting the EMBER feature set [3] to Android malwares, on a per-function basis. To check for storage access, we search for strings such as “/storage/” or “/sdcard/”. For the equivalent of registry access, the strings of interest are “/shared_prefs/”, “Settings.Secure”, “Settings.System”, and “Settings.Global”. MZ dropper is substituted with any sign of in-memory code execution, which exhibits in keywords such as “ClassLoader”, “DexFile”, “loadDex”, “loadClass”, “defineClass”, or “loadLibrary”.

We also utilize method information available to us from Androguard [12] analyzer getter functions. All numerical features are kept as is without normalization, and any string/string list features are converted into a 50-dimensional number vector using the hashing trick [52]. We list all extracted features in Tab. ?? . Note that only the first 5 features in the table are available across all methods: for example, we cannot extract any bytecode statistics from external functions as they are not defined/available in the extracted APK. These 5 features form the **Trim** variant as described in the main text.

A.3 Edge Features for Malware FCGs

For edge features, we note that the relationship between two functions is an invocation, and thus any information about it (e.g. passed parameters, return values) requires an inspection of the call stack, which is only available at run time [36]. As we do not conduct dynamic analysis in this work, we do not extract any edge features to enrich the FCG representation.

A.4 MalNet-Tiny Variants Specifications

We construct MalNet-Tiny-Common to have the same malware families but different malware types, to illustrate the final trained model’s ability to deal with covariate shift. We construct MalNet-Tiny-Distinct to have different malware families/types, to illustrate

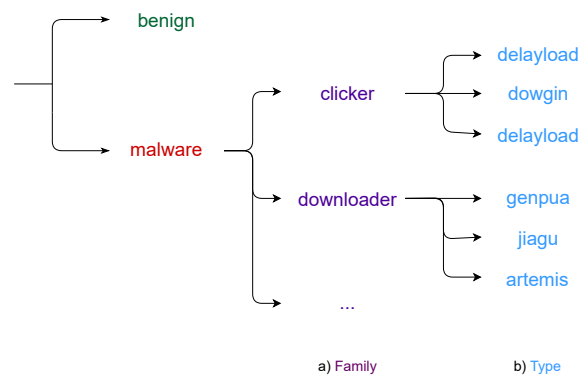


Fig. 4: Example of hierarchical malware labeling in MalNet.

Tab. 6: Specifications of all extracted function metafeatures.

	Feature	Type	Embedding
Names	Class name	String list ^[a]	Hashing trick
	Method name	String	Hashing trick
Method signature	Number of parameters	Integer	As-is
	Parameter types	String list	Hashing trick
	Return type	String	Hashing trick
Method misc.	Access flags	Binary ^[b]	Multi-hot
	Number of local registers	Integer	As-is
Code	Length	Integer	As-is
	Byte histogram	Integer list	Distribution ^[c]
	Byte-entropy histogram	Integer list	Distribution
Instructions	Length	Integer	As-is
	Opcode names	String list	Hashing trick
Strings	Contains invalid characters	Boolean	As-is
	String literal	String	Hashing trick
	Number of strings	Integer	As-is
	Average string length	Float	As-is
	Character histogram	Integer list	Distribution
	Character entropy	Float	As-is
	Number of external paths	Integer	As-is
	Number of URLs	Integer	As-is
	Number of IP addresses	Integer	As-is
	Registry modifications	Integer	As-is
In-memory executions	Integer	As-is	
Misc.	Are instructions cached?	Boolean	As-is

^a Class names are tokenized, e.g. ["java", "lang", "Object"]

^b The concerned flags are: public, private, protected, static, final, synchronized, bridge, varargs, native, interface, abstract, strictfp, synthetic, constructor.

^c The number list is normalized into a proper distribution.

the final trained model’s ability to deal with domain shift. The malware families/types are listed in Tab. 7.

For sample selection, we only select malwares with under 5000 nodes/functions to match with MalNet-Tiny. On malware type selection, there are two important details:

- With the benign class not having a different type (i.e. just *benign/benign*), where we select a disjoint set of malware samples from the original dataset.
- For some malware families, there are no subtype that has 1000 samples. To deal with this issue, we opt for including other subtypes with as little overlap as possible, denoted as *mixed* in Tab. 7.

While we have done our best to avoid label duplicates, it is unavoidable given the limitation of the original MalNet. We also believe that this labeling noise is not detrimental, as our classification results reach over 94% for both datasets.

B Detailed Experiment Setup

B.1 GNN Architectures

Depending on the model architecture, different feature collation schemes may be better or worse. For example, traditional message-passing graph neural networks propagate information from only the neighboring nodes, and thus may benefit from any additional features. In contrast, Transformer-based models can attend to all nodes in the graph (e.g. a global pseudonode), which may cause noisy features of an unrelated node to negatively affect the aggregation of another node’s features. Therefore, we experiment with different graph neural network architectures to see how they perform under different settings:

- Graph Convolutional Network (GCN) [35]: a traditional message-passing graph neural network that uses a convolutional operation to aggregate features from neighboring nodes.
- Graph Isomorphism Network (GIN) [56]: a more powerful message-passing architecture that can distinguish between different graph structures, based on the 1-WL test [53].

Tab. 7: Malware labels in MalNet-Tiny, MalNet-Tiny-Common, and MalNet-Tiny-Distinct.

MalNet-Tiny	MalNet-Tiny-Common	MalNet-Tiny-Distinct
addisplay/kuguo	addisplay/dowgin	spr/lootor
adware/airpush	adware/startapp	clicker++trojan/dowgin
benign/benign	benign/benign	riskware/nandrobox
downloader/jiagu	downloader: tencentprotect, openconnection, dowgin, genpua, hiddenapps, artemis	malware/sdi, tencentprotect, deepscan, fakeind, genpua, fwad, hiddenapps, oddjs, azshouyou, cve, jiagu
trojan/artemis	trojan/deng	spyware/smspay, ginmaster, genbl, wapsx, zwalls, opfake, lmmob, admogo, deng, adwo, axent, multiad, plankton, dowgin

- GPS [46]: a hybrid Transformer architecture that combines message-passing and attention mechanisms to capture both local and global information in the graph.
- Exphormer [47]: a sparse hybrid Transformer architecture that improves upon GPS via an improved attention mechanism, allowing better information propagation.

B.2 Adaptation Methods

We select these methods such that they do not alter the upstream training process, and cover a wide range of approaches. For test-time adaptation methods:

- Tent [50]: a generic approach that finetunes only the normalization layers per inference.
- T3A [31]: a generic approach collecting inferred samples’ embeddings as class prototypes to replace the original classifier weights.
- GTrans [32]: graph TTA for node classification that augments input graphs to optimize a surrogate loss, which we adapted to work with the graph level.

For domain adaptation approaches, we select the following baselines:

- k-NN Probe: utilizes the k-NN classifier fitted to the finetuning dataset to probe the model’s predictions on the downstream task, and replaces the classifier head with a k-NN classifier [10].
- Finetuning: fully finetunes the model on the downstream dataset for a few epochs, a common approach in transfer learning [11, 44].
- AdapterGNN [37]: a graph-specific parameter-efficient finetuning method which adds an adapter to each message passing layer, and finetunes only the adapters’ parameters.

While there are newer TTA/DA approaches for GNN (e.g. [5]), they either do not provide the source code, or requires specific architectural properties, rendering them generally inapplicable.

B.3 Implementation Modifications

B.3.1 Readout function. After message-passing, we use the global max pooling operation to aggregate the node features into a single graph-level representation, as is also used in the Transformer-based architectures [46, 47]. This readout choice has a nice interpretation: a program is the product of all its functions, and thus if one function behaves like a malware, the whole program is likely malicious.

This is in contrast to the more traditional global mean pooling operation, which may dilute the effect of a single malicious function by averaging it with other benign functions.

B.3.2 Classifier initialization. Across all experiments on MalNet-Tiny-Common, we start finetuning on the checkpoint as is. For MalNet-Tiny-Distinct, we reinitialize the classifier head for finetuning-based methods, as the model cannot adapt to new malware families without retraining the classifier.

B.3.3 Prune. For *Prune*, we omit removing isolated nodes during data preparation to prevent empty graphs. This is because for some malwares, all of its code-containing functions do not call each other (and e.g. only call APIs), and thus become completely isolated after all other nodes are pruned.

B.3.4 GTrans. We adapt the method as-is to graph classification by keeping all perturbation schemes and hyperparameters unchanged from the original code onto our graph classifiers, which only differ from their node classifying models in that the former has a readout step before classification. The only exception is that we disabled adjacency perturbation, as some graph architectures did not support edge features. While the original work did not experiment on graph classification, it mentioned that the method can theoretically be applied to the setting [32], motivating us to adapt it to our problem.

B.4 Hardware and Implementation

All experiments are conducted on a single NVIDIA RTX 6000 Ada with 48Gb of memory. All runs are seeded with the same seed for reproducibility, using the hyperparameter configurations listed in the original paper [46, 47] for a fair comparison. Each of our experiment takes 1-2 hours to run, depending on the model architecture in use.

C Additional Experiment Results

C.1 Different LLM Options

In this section, we conduct our evaluations with different LLMs for feature extractions. Besides CodeXEmbed [38] (CXE) which is the only LLM that satisfies all of our requirements, we also experiment with UniXcoder [22] (UniX), which is a code-specific LLM embedder with a much smaller context window of 512; and Qwen 3 [57], a multi-domain LLM which can support data in code domain with a larger context.

Distribution Shifts in Graph-Based Android Malware Classification

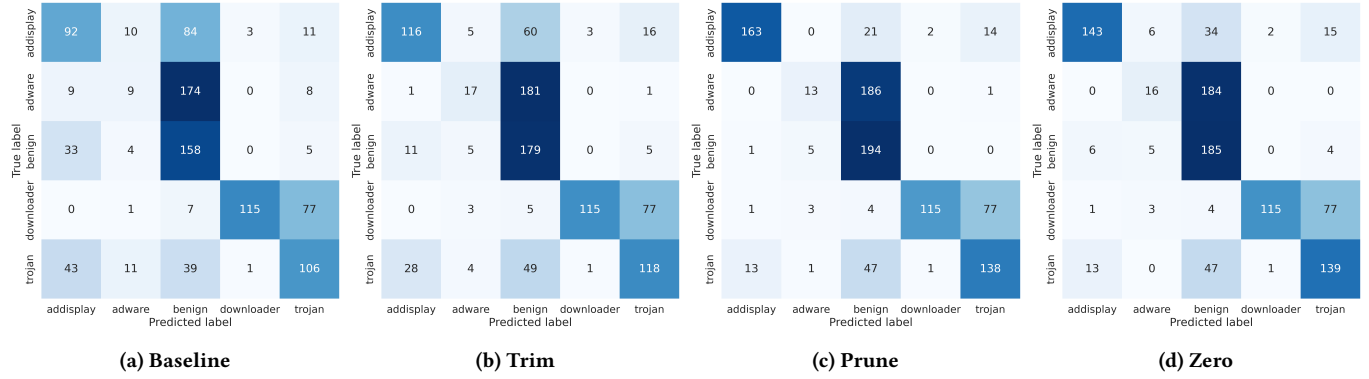


Fig. 5: Confusion matrices on MalNet-Tiny-Common for GCN across different feature construction schemes.

Tab. 8: Models’ accuracy on MalNet-Tiny and MalNet-Tiny-Common across different LLM embedding models. Subscript denotes standard deviation over 3 independent runs. Best result in bold, second best underlined.

Method	Features			GCN		GIN		GPS		Expformer	
	Meta	LLM	LDP	Tiny	Cmn.	Tiny	Cmn.	Tiny	Cmn.	Tiny	Cmn.
Prune	-	CXE	-	94.33 _{0.24}	60.30 _{1.98}	94.30 _{0.43}	61.10 _{0.22}	94.77 _{0.26}	53.50 _{2.12}	94.50 _{0.22}	55.27 _{0.66}
	-	UniX	-	93.93 _{0.21}	54.90 _{0.85}	94.17 _{0.33}	58.77 _{1.94}	94.47 _{0.25}	56.43 _{1.08}	94.70 _{0.22}	54.93 _{0.50}
	-	Qwen3	-	94.57 _{0.12}	55.23 _{2.08}	94.50 _{0.33}	59.97 _{0.54}	94.60 _{0.37}	54.57 _{1.04}	95.13 _{0.39}	53.27 _{1.20}
	-	CXE	✓	94.33 _{0.29}	58.33 _{1.72}	94.83 _{0.42}	59.97 _{0.95}	94.80 _{0.28}	53.07 _{0.73}	94.97 _{0.52}	54.87 _{1.52}
	-	UniX	✓	94.13 _{0.29}	55.23 _{0.69}	94.63 _{0.57}	56.63 _{0.69}	94.73 _{0.52}	56.53 _{0.56}	94.53 _{0.42}	55.27 _{0.95}
	-	Qwen3	✓	93.87 _{0.52}	57.57 _{1.38}	94.53 _{0.37}	58.43 _{1.08}	95.17 _{0.12}	54.07 _{0.95}	94.90 _{0.33}	52.57 _{1.45}
	✓	CXE	-	95.17 _{0.33}	59.70 _{0.41}	94.20 _{0.24}	61.63 _{2.19}	94.87 _{0.41}	55.57 _{1.52}	95.00 _{0.43}	52.37 _{0.12}
	✓	UniX	-	94.47 _{0.24}	53.73 _{1.09}	93.90 _{0.08}	54.97 _{0.73}	94.20 _{0.14}	54.30 _{0.22}	94.60 _{0.29}	52.93 _{0.83}
	✓	Qwen3	-	94.10 _{0.51}	55.60 _{1.07}	94.27 _{0.31}	59.13 _{0.25}	94.97 _{0.33}	54.73 _{0.98}	93.87 _{1.11}	52.00 _{0.78}
	✓	CXE	✓	94.23 _{0.09}	57.03 _{1.08}	94.70 _{0.08}	60.07 _{1.67}	94.77 _{0.21}	56.70 _{0.93}	94.97 _{0.31}	53.93 _{1.05}
	✓	UniX	✓	94.43 _{0.31}	55.73 _{1.41}	93.50 _{0.16}	55.33 _{0.45}	94.90 _{0.37}	52.50 _{1.20}	93.87 _{1.07}	53.23 _{1.47}
	✓	Qwen3	✓	95.27 _{0.17}	57.00 _{2.00}	94.53 _{0.49}	57.40 _{0.36}	94.80 _{0.22}	55.07 _{1.68}	94.67 _{0.29}	51.87 _{1.35}
Zero	-	CXE	-	94.60 _{0.22}	56.70 _{2.03}	94.27 _{0.26}	58.60 _{1.70}	95.10 _{0.36}	56.73 _{0.54}	94.60 _{0.43}	55.57 _{1.58}
	-	UniX	-	94.30 _{0.36}	56.17 _{1.43}	94.67 _{0.19}	58.07 _{1.52}	94.40 _{0.41}	55.17 _{0.09}	94.60 _{0.29}	56.07 _{1.06}
	-	Qwen3	-	94.47 _{0.45}	57.93 _{0.82}	94.80 _{0.00}	57.93 _{2.25}	95.03 _{0.40}	54.07 _{2.00}	94.50 _{0.36}	55.70 _{2.09}
	-	CXE	✓	94.57 _{0.41}	58.60 _{1.19}	94.50 _{0.36}	56.57 _{0.34}	94.60 _{0.37}	54.87 _{1.39}	95.00 _{0.22}	55.33 _{2.33}
	-	UniX	✓	94.47 _{0.17}	53.30 _{0.50}	94.37 _{0.37}	57.60 _{1.19}	94.73 _{0.62}	53.87 _{1.86}	94.47 _{0.58}	54.27 _{0.74}
	-	Qwen3	✓	93.97 _{0.21}	56.13 _{0.91}	94.30 _{0.54}	57.33 _{0.21}	95.03 _{0.45}	53.93 _{2.04}	94.63 _{0.12}	51.77 _{1.51}
	✓	CXE	-	93.80 _{0.16}	58.87 _{1.46}	94.93 _{0.34}	56.33 _{0.62}	95.27 _{0.21}	54.97 _{1.48}	94.97 _{0.47}	55.87 _{0.31}
	✓	UniX	-	93.90 _{0.51}	52.53 _{1.19}	94.87 _{0.09}	56.13 _{0.33}	94.03 _{0.37}	52.00 _{1.49}	94.47 _{0.39}	55.83 _{1.43}
	✓	Qwen3	-	94.43 _{0.29}	53.97 _{1.21}	94.87 _{0.39}	59.23 _{0.66}	94.33 _{0.33}	55.77 _{1.62}	94.17 _{0.09}	54.03 _{0.45}
	✓	CXE	✓	94.37 _{0.37}	59.00 _{0.86}	94.93 _{0.29}	59.10 _{0.67}	94.53 _{0.09}	53.60 _{0.67}	94.40 _{0.08}	54.73 _{1.43}
	✓	UniX	✓	94.30 _{0.22}	53.37 _{1.09}	94.10 _{0.29}	56.60 _{1.12}	94.43 _{0.29}	54.90 _{1.02}	93.63 _{0.21}	54.90 _{0.64}
	✓	Qwen3	✓	93.67 _{0.05}	53.23 _{0.45}	94.63 _{0.24}	57.13 _{0.78}	94.73 _{0.54}	53.30 _{2.12}	94.97 _{0.42}	55.70 _{1.53}

The complete ablation results are reports in Table 8, in which CXE outperforms the other LLMs across most variants of the pipeline as we expected. We thus opt for CodeXEmbed as the default option for our method.

Tab. 9: Inference time of different architectures on MalNet-Tiny-Features when comparing to original structure-only baseline.

Method	GCN	GIN	GPS	Exphormer
Baseline	1x	1x	1x	1x
Trim	1.31x	1.47x	1.02x	1.12x
Prune	2.65x	3.69x	1.12x	1.24x
Zero	4.51x	6.20x	1.25x	2.34x

C.2 Pipeline Running Time

Table 9 reports the comparative evaluation time across different variants of our approach. The multipliers are as expected: GCN layer only include a matrix multiplication, which scales linearly with the number of features; while GIN scales quadratically due to having an MLP at every layer. The Transformer architectures, in contrast, have a feature downscaler very early on before the main computational-heavy components, and thus the difference in overhead with respect to dimension size is much more negligible.

It may come across that these evaluation times seem too fast given our feature set can be very large (upto 651x vs. the baseline for our largest variant). This efficiency is thanks to the approaches of our method in dealing with non-universal features, which take up a large portion of the feature matrix. Specifically, *Prune* removes up to 89.60% of nodes that do not have all available features (even when it keeps full-featured isolated nodes while the other datasets have them removed); and *Zero* creates a sparse matrix with up to 89.09% of zeros per node. These properties drastically reduce the amount of computation needed for such a high-dimensional input to the models.

C.3 Pipeline Configuration Selection

Tab. 10: Optimal pipeline configuration for highest accuracy on distribution-shifted evaluation for different architectures.

Architecture	Method	Meta	LLM	LDP
GCN	Prune	-	CXE	-
	Zero	✓	CXE	✓
GIN	Prune	-	CXE	-
	Zero	✓	Qwen3	-
GPS	Prune	✓	CXE	✓
	Zero	-	CXE	-
Exphormer	Prune	-	CXE	-
	Zero	-	UniX	-

From the complete result tables, we take the means of all the accuracy results per each variant. From that aggregation, we provide the best configuration in terms of accuracy for each model architecture in Table 10. For a simpler recommendation that works generally well across all settings, the configuration with the best overall classification performance is LLM feature-only with CodeX-Embed.

D Further Discussion on Related Works

D.1 Graph Representations for Android Malwares

Before the the release of MalNet, *αCyber* [27] devised a graph-based feature extraction on malware metadata, representing all available data as one giant heterogeneous graph. This approach was not generalizable due to the exploding space complexity, and that the authors worked on a private propriety dataset. AMDroid [19] proposed to use function call graphs (FCGs) as the graph representation of Android malwares, but uses a random-walk based feature extraction method instead of a graph neural network (GNN). Alasmay et al. [1] extracted a Control Flow Graph as the representation instead, and focused on the Internet-of-Thing domain. CGDroid [14] proposed training a word2vec [42] embedding model for bytecode, with manual annotation of API security levels and permission lists as hints for the model to work with. HyGNN-Mal [59] took a different approach and extracted the abstract syntax tree as the graph representation. BejaGNN [15] also used word2vec to generate features, but instead utilized inter-procedural control flow graph to for the graph structure.

D.2 Distribution Shift for Graph Machine Learning

To alleviate the effect of distribution shift in graph machine learning, a number of methods have been proposed. Some approaches are finetuning-based, which update the model parameters to adapt to the new distribution – latest development have been focusing on being parameter-efficient through the use of an adapter [21, 37]. Others worked on domain adaptation techniques, such as applying self-supervised learning on a pretrained model at test-time [9, 51], or adapting the input graphs themselves to match the learned training distribution [28, 32, 34]. A more novel approach to graph adaptation is graph prompt tuning, which uses a prompt to adapt the model to the new distribution without modifying the model parameters [13, 18, 39, 49]. However, similar to prompt tuning in natural language processing, these methods typically require pretraining on a large corpus of graphs; thus, they are not applicable to many graph classification problems with limited training data.